Anisotropy of magnetohydrodynamic turbulence at low magnetic Reynolds number

Anatoliy Vorobev and Oleg Zikanov[a)]
University of Michigan–Dearborn, Dearborn, Michigan 48128-1491

Peter A. Davidson
University of Cambridge, Cambridge CB2 1PZ, United Kingdom

Bernard Knaepen
Universite Libre de Bruxelles, B-1050 Brussels, Belgium

(Received 8 July 2005; accepted 25 October 2005; published online 13 December 2005)

Turbulent fluctuations in magnetohydrodynamic flows are known to become anisotropic under the action of a sufficiently strong magnetic field. We investigate this phenomenon in the case of low magnetic Reynolds number using direct numerical simulations and large eddy simulations of a forced flow in a periodic box. A series of simulations is performed with different strengths of the magnetic field, varying Reynolds number, and two types of forcing, one of which is isotropic and the other limited to two-dimensional flow modes. We find that both the velocity anisotropy (difference in the relative amplitude of the velocity components) and the anisotropy of the velocity gradients are predominantly determined by the value of the magnetic interaction parameter. The effects of the Reynolds number and the type of forcing are much weaker. We also find that the anisotropy varies only slightly with the length scale. © *2005 American Institute of Physics*.
[DOI: 10.1063/1.2140847]

I. INTRODUCTION

Magnetohydrodynamic (MHD) turbulent flows are ubiquitous in the universe, occurring in numerous astrophysical, geophysical, and technological applications. It is known that turbulent fluctuations become anisotropic in the presence of a sufficiently strong magnetic field, which has important consequences for the properties of the turbulence and possibly requires a modification of the numerical models applied to such flows. Specific manifestations of the anisotropy may vary but the principal mechanism is always an elongation of the flow structures (turbulent eddies) along the lines of the magnetic field.

The main difference between the kinds of MHD turbulence is due to different values of the magnetic Reynolds number

$$\mathrm{Re}_m \equiv \frac{vL}{\eta}, \tag{1}$$

where $\eta=(\sigma\mu_0)^{-1}$ is the magnetic diffusivity, σ and μ_0 being the electric conductivity of the liquid and the magnetic permeability of vacuum, and v, L are the typical velocity and length scale of the flow. If $\mathrm{Re}_m \gtrsim 1$, there is a two-way coupling between the fluctuations of the magnetic field and the velocity (see, e.g., Refs. 1 and 2). As the fluid moves in the applied magnetic field **B**, induced electric currents result in the Lorentz force affecting the flow and in the modification of the imposed field by perturbations **b** of comparable or even larger amplitude. This happens, for example, in astrophysical processes (in stars, the interstellar medium, etc.), where $\mathrm{Re}_m \gg 1$, and in geophysics (the geodynamo), where $\mathrm{Re}_m \sim 10^2$. A discussion of the anisotropy effects at large magnetic Reynolds number can be found, for example, in Ref. 3.

The opposite case of $\mathrm{Re}_m \ll 1$ occurs in the majority of technological processes, where a strong steady magnetic field is imposed on an electrically conducting liquid. Examples include the continuous casting of steel and aluminum, the growth of semiconductor crystals, and lithium cooling blankets proposed for future fusion reactors. In this case, the low-Re_m (so-called quasistatic) approximation can be applied.[1,2] Since the diffusion time $T_d \equiv L^2/\eta$ of the magnetic field is much smaller than the eddy turnover time $T \equiv L/v = T_d/\mathrm{Re}_m$, we can assume that the magnetic field fluctuations **b** associated with the fluid motion adjust instantaneously to the velocity fluctuations and are given by the formula

$$\Delta\mathbf{b} = -\frac{1}{\eta}(\mathbf{B}\cdot\nabla)\mathbf{v}, \tag{2}$$

where **v** is the velocity field. Furthermore, it can be shown that the fluctuations **b** are much weaker than the imposed field **B** and, thus, can be neglected in the expressions for the Lorentz force and Ohm's law. One can say that the coupling between the velocity and the magnetic field is one-way since the former does not cause any substantial modification of the latter.

At small Re_m, one can simplify the system of governing equations using the fact that the rotational part of the Lorentz force reduces to a linear functional of the velocity

[a)]Electronic mail: zikanov@umd.umich.edu

$$\mathbf{F}[\mathbf{v}] = -\frac{\sigma B^2}{\rho}\Delta^{-1}\frac{\partial^2 \mathbf{v}}{\partial z^2}, \tag{3}$$

where ρ is the density of the fluid, Δ^{-1} is the reciprocal Laplace operator, and we assume that the imposed constant magnetic field is uniform and vertical $\mathbf{B}=B\mathbf{e}_z$.

The validity of the quasistatic approximation has been established in numerous theoretical, experimental, and numerical investigations. For homogeneous turbulence, comparison between numerical solutions of quasistatic and full MHD equations[4] showed that the approximation provides accurate results at $\mathrm{Re}_m \leqslant 1$, i.e., even when the condition of smallness of Re_m is not strictly fulfilled. From the computational viewpoint, use of full MHD equations at small Re_m is not just unnecessary but also impractical since it leads to severe limitations on the time step needed to resolve two time scales, very small magnetic diffusion time T_d, and much larger eddy turnover time T.[4]

The flow transformation under the impact of the Lorentz force (3) has been actively studied in analytical,[5–8] experimental,[9,10] and numerical[11–13] works. The papers mentioned above represent only a fraction of the literature on the subject, further references being available therein. Far from walls, the action of the magnetic field is twofold. First, the induced electric currents result in an additional dissipation of the kinetic energy via Joule dissipation. Second, as was mentioned above, the flow becomes anisotropic, its structures being elongated along the magnetic field lines.

The reason for the anisotropy becomes especially transparent if one assumes that the flow is unbounded and uniform and uses the Fourier representation. The Fourier transform of (3) is[14]

$$\hat{\mathbf{F}}[\hat{\mathbf{v}}] = -\frac{\sigma}{\rho}\frac{(\mathbf{B}\cdot\mathbf{k})^2}{k^2}\hat{\mathbf{v}}(\mathbf{k},t) = -\frac{\sigma B^2}{\rho}\hat{\mathbf{v}}(\mathbf{k},t)\cos^2\theta, \tag{4}$$

where $\mathbf{k}$ is the wave-number vector and θ is the angle between $\mathbf{k}$ and $\mathbf{B}$. The rate of the Joule dissipation of a Fourier mode with the wave-number vector $\mathbf{k}$ is

$$\mu(\mathbf{k}) = \frac{\sigma B^2}{\rho}[\hat{\mathbf{v}}(\mathbf{k},t)\cdot\hat{\mathbf{v}}^*(\mathbf{k},t)]\cos^2\theta, \tag{5}$$

where * stands for complex conjugate, so the dissipation is anisotropic. It attains its maximum for the Fourier modes with $\mathbf{B}\|\mathbf{k}$ and is zero for the modes with $\mathbf{B}\perp\mathbf{k}$, i.e., for the modes independent of the z coordinate. The dissipation tends to eliminate velocity gradients in the direction of $\mathbf{B}$ and elongate the flow structures in this direction. The limiting case is a two-dimensional state completely independent of the z coordinate. The magnetic field fluctuations, electric currents, and Joule dissipation are all equal to zero in this state.

This picture of the flow transformation was first given in Ref. 5. A remarkable feature of the picture is that, according to (5), the relative rate of the dissipation $\mu(\mathbf{k})/\hat{\mathbf{v}}^2$ depends on the angle θ but not on the wave number k. One is thus tempted to assume that equal anisotropy develops at all length scales in the flow. The situation, however, looks more complicated if we take into account the nonlinearity of the Navier-Stokes equations and the resulting energy transfer between the modes, which tends to restore isotropy. An estimate of the ratio between the Lorentz force and the nonlinear term in the momentum equation is given by the magnetic interaction parameter

$$N \equiv \frac{\sigma B^2 L}{\rho v}. \tag{6}$$

There is a subtlety concerning the fact that, according to (3), the actual ratio between the Lorentz and inertia forces should include L^3/L_z^2 in place of L. As the flow becomes anisotropic, L_z grows and the ratio decreases. Although the decrease reflects the real fact that the Lorentz force and Joule dissipation become weaker in the anisotropic state and cease to exist in a two-dimensional flow, it is customary to set N to a constant value calculated using (6) with L taken at a certain state of the flow. For example, in the discussion of our results in the following sections, L is the integral length scale of the isotropic turbulent flow just before the introduction of the magnetic field.

The linearized picture of the flow development[5] is rigorously correct only in the limit of $N \gg 1$, when the inertia force is negligible in comparison with the Lorentz force. At a finite value of N, one can expect a more complex scenario, probably with a scale-dependent anisotropy.

Another way to arrive at the same suggestion is to notice that, while the Joule damping time $\tau \equiv \rho/\sigma B^2$ is independent of the typical length scale ℓ, the eddy turnover time $T=\ell/v$ is, generally, not. The magnitude of the scale-related magnetic interaction parameter $N(\ell)=T/\tau$ can vary with the scale and so can the flow anisotropy. $N(\ell)$ can be estimated assuming $\ell \sim 1/k$ and using $v \sim [\mathrm{kE}(k)]^{1/2}$ for the typical velocity scale. It is easy to see that, within the inertial range, $N \sim \ell^{2/3}$ in the isotropic case and $N \sim \ell^0$ in the case of a two-dimensional flow. In the dissipative subrange, the energy of both isotropic and anisotropic flows decreases faster with decreasing ℓ than in the inertial range, which implies faster decrease of $N(\ell)$.

Here, we would like to mention an analogy with the cases of stratified, rotating, or highly strained turbulence. For example, it is generally believed that the Kolmogorov picture of the turbulent fluctuations becoming isotropic at small scales, regardless of the details of the large-scale behavior, is still valid for rotating flows since the Rossby number becomes negligible at small scales. One example is atmospheric turbulence, which is isotropic at the small-scale level. We have to note, however, that the Reynolds number must be large for this effect to become visible. For example, recent moderate-Re simulations[15] of rotating and stably stratified turbulence showed anisotropy down to the smallest scales.

There is less agreement regarding the scale dependence of the anisotropy in shear flows. On the one hand, there is an experimental confirmation of the Kolmogorov hypothesis.[16] On the other hand, a growing number of studies point to a persistent small-scale anisotropy in homogeneous shear flows.[17,18] Here, again, one has to separate the experimental and theoretical results dealing with flows at very large Reynolds numbers from numerical simulations inevitably limited

to small or moderate Re. Our results presented below belong to the latter group and, thus, cannot serve for support or invalidation of the Kolmogorov hypothesis in the case of MHD turbulence.

For low-Re_m MHD turbulence, the question of anisotropy at different length scales has recently become particularly interesting in view of attempts to apply traditional large eddy simulation (LES) models.[19] Calculations of decaying turbulence at $N \leqslant 10$ showed a good agreement between the flows obtained with the dynamic Smagorinsky model[20,21] and with direct numerical simulations (DNS). This result, however, is not entirely convincing since the hydrodynamic Reynolds number in these simulations is not very high ($\mathrm{Re}=380$ and $\mathrm{Re}_\lambda=84$ at the beginning of the examined decay period). With the added impact of strong Joule dissipation, the decaying flows were only weakly turbulent in the interesting case of a strong magnetic field. The subgrid-scale (SGS) model was, therefore, responsible for only a small fraction of the energy dissipation. One may anticipate worse agreement at higher Re when the SGS model is required to absorb a larger fraction of the total dissipation since, generally, it can be expected that the LES models developed under the assumption of local isotropy perform poorly in the case of a strongly anisotropic MHD flow.

In this paper, we investigate the anisotropy of low-Re_m MHD turbulence using the DNS and LES of a forced flow in a box with the periodic boundary conditions. The geometry of the computational domain, LES model, forcing algorithm, and other details of the numerical experiments are described in Sec. II. The main results of the paper are presented in Sec. III, where we discuss the flow anisotropy. Concluding remarks are provided in Sec. IV.

II. MODEL AND NUMERICAL EXPERIMENTS

A. Governing equations, forcing, and LES model

We consider the flow of a viscous, incompressible, electrically conducting fluid in the presence of a constant uniform magnetic field $\mathbf{B}=B\mathbf{e}_z$. The quasistatic approximation is used and the Lorentz force is given by (3). After applying $\boldsymbol{\nabla}\times[\boldsymbol{\nabla}\times\ldots]$ to eliminate pressure and taking the Fourier transform, the governing equations (in dimensional form) become

$$\frac{\partial\hat{\mathbf{v}}}{\partial t}(\mathbf{k},t)=-\frac{1}{k^2}[\mathbf{k}\times(\mathbf{k}\times\hat{\mathbf{q}})]-\left[\nu\mathbf{k}^2+\frac{\sigma B_0^2}{\rho}\left(\frac{k_z}{k}\right)^2\right]\hat{\mathbf{v}}+\hat{\mathbf{f}}(\mathbf{k}),$$
$$\mathbf{k}\cdot\hat{\mathbf{v}}=0, \tag{7}$$

where ν is the kinematic viscosity, $\hat{\mathbf{q}}$ is the Fourier transform of the nonlinear term, and $\hat{\mathbf{f}}$ is the forcing term discussed below.

The flow is calculated in a rectangular box with periodic boundary conditions. Since we expect elongation of turbulent structures along the z axis, an elongated box of dimensions $2\pi\times2\pi\times4\pi$ is used. This does not entirely eliminate the effect of the artificial periodic boundaries that occur at large N, when the typical vertical scale of the flow grows so that it becomes comparable with the box size (see Fig. 4 for an illustration). The purpose is to provide larger separation between the length scales directly affected by the boundary conditions and the small scales, the anisotropy of which is the focus of our investigation.

Equation (7) is solved by a standard pseudospectral code using a fourth-order, low-storage, time-integration scheme.[22] Nonlinear terms are evaluated in real space after backward Fourier transform of the velocity field. In order to remove aliasing errors, the method of phase-shifting is used.[23] In this method, products are computed on eight appropriately shifted physical grids and the aliasing contributions are eliminated by taking averages of those products. In Fourier space, this corresponds to considering successively eight phase-shifted versions of the velocity field during each time step.

Most previous studies of the effect of applied magnetic field on low-Re_m turbulence considered freely decaying flows.[5,7,9–11] Albeit a mathematically neat model for the process of suppression of turbulence by a magnetic field, this formulation is at odds with the situation in many real flows, where there is a steady energy input into large scales. For example, in continuous steel casting or in crystal growth, a constant level of turbulence is maintained by, respectively, nozzle jets or wall rotation and convection. Further difficulty associated with the decay model is that the statistical properties of the flow cannot be reliably quantified in numerical simulations. Since our goal in this paper is precisely such quantification (especially of the anisotropy characteristics), we chose to work with the model of forced flow. An artificial forcing is applied at the large length scales to simulate the energy input in real systems and generate a statistically steady flow over a long period of time.

An applied force with the Fourier transform

$$\hat{\mathbf{f}}(\mathbf{k})=\begin{cases}\alpha(\mathbf{k})\hat{\mathbf{v}}(\mathbf{k}) & \text{if } 1.5\leqslant k\leqslant 3.1,\\ 0 & \text{otherwise,}\end{cases} \tag{8}$$

appears in (7). This choice results in a flow with the integral length scale $L=\pi/(2v^2)\int_0^\infty k^{-1}E(k)dk$, equal, in the nonmagnetic case, to approximately $1/9$ of the smaller dimension of the computational domain. The time-dependent coefficients $\alpha(\mathbf{k})$ are determined at each time step in such a way that the network by the forcing is equal to a constant dissipation rate ϵ_0. After a short initial development, the flow reaches an equilibrium state with approximately constant energy and the total (viscous plus magnetic) dissipation rate oscillating only slightly around ϵ_0.

Two types of forcing are used. In one, the forcing is isotropic in the sense that the work is equally divided among the forced modes by choosing

$$\alpha(\mathbf{k})=\frac{\epsilon_0}{N_{\mathrm{forced}}[\hat{\mathbf{v}}(\mathbf{k})\cdot\hat{\mathbf{v}}^*(\mathbf{k})]}, \tag{9}$$

where N_{forced} is the number of modes subject to the forcing. This always keeps the forced modes chaotic and three-dimensional even though they can acquire significant anisotropy through the action of the magnetic field. An advantage of using (9) over similar forcing schemes with $\mathbf{k}$ independent α is that, with the latter, the energy input into each forced mode is proportional to its amplitude. This can lead to the

development of a pseudolaminar flow such as in Ref. 12, with the entire energy input limited to a single mode. Although interesting, such dynamics would interfere with pursuing the main goal of our paper, the investigation of anisotropy of turbulent fluctuations.

We realize that there is always a question of the impact of an artificial three-dimensional forcing or, in general, of the behavior of the large-scale energetic modes on the development of the anisotropy at smaller scales. To investigate this effect, we perform an additional series of simulations with a purely two-dimensional forcing. Formulas (8) and (9) remain valid but the forcing is limited to the modes with $k_z=0$. This forcing imposes its own anisotropy at large scales.

The method of direct numerical simulation can only be applied to the flows with low to moderate Reynolds numbers. This presents an inevitable problem of limiting our conclusions to the case of turbulence of low intensity. In order to investigate the possible effect of the Reynolds number on the anisotropy, numerical experiments at higher Re are carried out using the LES approach based on the standard dynamic Smagorinsky model.[20,21] Although, as we discuss in Sec. I, the applicability of the traditional LES models to MHD turbulence is not obvious, we can justify the use of such a model in our study by the results of an *a posteriori* DNS versus LES comparison. Such a test was initiated in Ref. 19 and is extended in this paper. We shall see that the dynamic model can be reasonably accurate (at least, as accurate as for the conventional hydrodynamic flows) in the simulations of the homogeneous MHD turbulence at moderate Re. The general question of the extent to which the imperfections of the LES model affect the effective Reynolds number of the flow is beyond the scope of our study and is not discussed in the paper.

B. Numerical experiments

Each experiment is staged as follows (see Fig. 1 for an illustration). First, a fully developed nonmagnetic turbulent flow is calculated by starting with a random, isotropic velocity field and then continuing the simulation at zero magnetic field for a sufficiently long period. This transitional period is judged complete when the values of the total kinetic energy and viscous and magnetic dissipation rates, defined as

$$E=\sum_{\mathbf{k}} E(\mathbf{k}), \quad E(\mathbf{k})=\frac{1}{2}[\mathbf{v}(\mathbf{k})\cdot\mathbf{v}^{*}(\mathbf{k})], \tag{10}$$

$$\epsilon=\nu\sum_{\mathbf{k}} k^2E(\mathbf{k}), \quad \mu=\frac{\sigma B_0^2}{\rho}\sum_{\mathbf{k}}\frac{k_z^2}{k^2}E(\mathbf{k}), \tag{11}$$

settle down to constant values. At the end of this period, the DNS flow has the integral length scale $L(t_0)=0.73$ and the root-mean-square velocity of turbulent fluctuations $v(t_0)=\sqrt{2/3E(t_0)}=0.91$. Similar values are obtained in the LES experiments (see Table I).

The flow field computed at the instant t_0 is used as a common initial condition for three simulations with different strengths of the magnetic field. For one of them, the magnetic field is absent. For the other two, referred to as the cases of moderate and strong magnetic field, the values of $\sigma B_0^2/\rho$ are chosen so that the magnetic interaction parameter (6) at $t=t_0$ is $N_0\approx 1$ and $N_0\approx 5$, respectively.

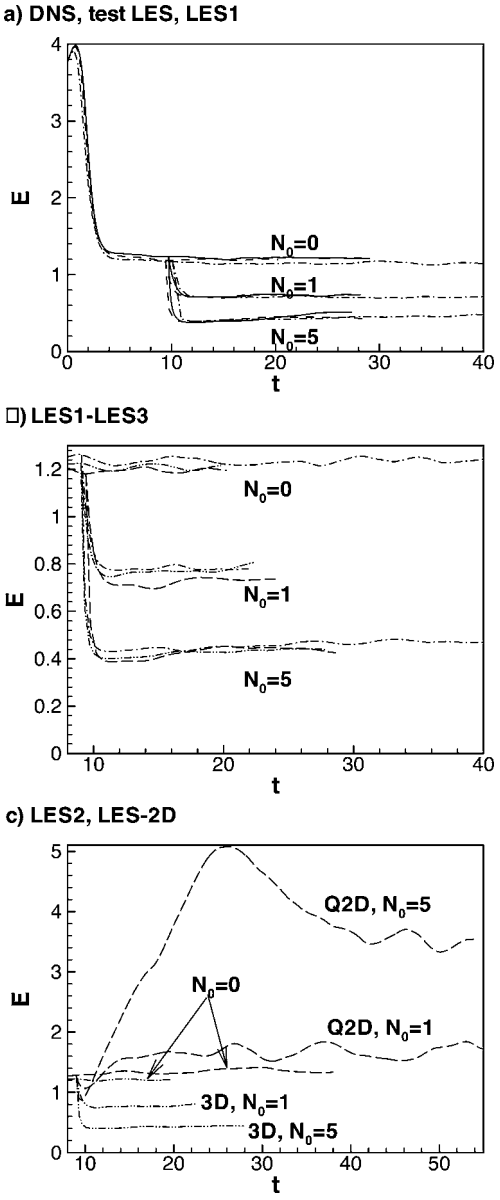

FIG. 1. Evolution of the total energy. (a) DNS (—), test LES1 (-·-·-), and LES1 (– – –). (b) LES1 (– – –), LES2 (-·····), and LES3 (-·-·-). (c) LES2 (-·····) and LES-2D (– – –). The time unit is approximately one eddy turnover time $T=L/u$ calculated for the isotropic flow at $t=t_0$.

We use the same value $\epsilon_0=0.5$ of the energy injection rate in every numerical experiment and adjust the viscosity coefficient ν to modify the integral length and Taylor microscale Reynolds numbers (the latter is believed to be a better measure of the intensity of turbulence, especially in the homogeneous flows such as grid turbulence or our periodic flow)

$$\mathrm{Re}=\frac{vL}{\nu}, \quad \mathrm{Re}_\lambda=\frac{v\lambda}{\nu}, \quad \lambda=\left(\frac{15\nu v^2}{\epsilon_0}\right)^{1/2} \tag{12}$$

shown in Table I for $t=t_0$. The table also presents the product of the maximum wave number $k_{\max}$ and the Kolmogorov

TABLE I. Summary of the parameters of the numerical experiments.

Run	$N_x \times N_y \times N_z$	$\nu \times 10^3$	$\mathrm{Re}_\lambda(t_0)$	$\mathrm{Re}(t_0)$	$k_{\max}\eta$	$L(t_0)$	$v(t_0)$	Line
(DNS)	$256\times256\times512$	2.2	94	302	1.6	0.73	0.91	—
(Test LES)	$32\times32\times64$	2.2	91	324	0.24	0.81	0.88	-·-·-
(LES1)	$64\times64\times128$	2.2	93	287	0.42	0.71	0.89	– – –
(LES2)	$64\times64\times128$	1	140	630	0.26	0.70	0.90	-·-·-·-
(LES3)	$64\times64\times128$	0.25	290	2620	0.12	0.72	0.91	-·-·-
(LES4)	$128\times128\times256$	0.25	290	2550	0.20	0.70	0.91	—
(LES-2D)	$64\times64\times128$	1	150	716	0.26	0.77	0.93	– – –

dissipation length $\eta=(\nu^3/\epsilon_0)^{1/4}$. In DNS, $k_{\max}\eta \geqslant 1.5$ was proven to be sufficient for accurate representation of the smallest scales of the flow. In LES, the value of this parameter can be considered as an indicator of the percentage of dissipation rate absorbed by the SGS model. The number of the Fourier modes used for the calculations varies between $N_x \times N_y \times N_z = 256\times256\times512$ for the DNS and $32\times32\times64$ for the lowest resolution LES.

The motivation for our LES experiments is as follows. Test LES and LES1 are carried out at the same Re as DNS and used as a test of the accuracy of the subgrid-scale model. LES1-LES3 are performed with gradually increasing Re, the purpose being to see if the anisotropy of LES flows changes when the Reynolds number is increased and the SGS model is forced to absorb an increasing fraction of the total dissipation. The goal of LES4 is to examine the anisotropy at the highest Re in a wider scale range than available in LES3. Comparison between LES3 and LES4 also provides a further opportunity to test the accuracy of the LES model. Finally, to investigate the influence of the large-scale forcing on the flow characteristics, LES-2D is carried out, in which the quasi-2D forcing is employed, but all the other parameters are identical to LES2.

C. Flow evolution

The evolution of the total energy and the rates of viscous and magnetic dissipation is shown in Figs. 1 and 2. Time is measured in dimensional units throughout the paper. Using the values of L and v in the developed isotropic flows at $t=t_0$ (see Table I), we can estimate the typical eddy turnover times as $T\approx0.8$. It can be seen that the periods of initial development and adjustment after the introduction of the magnetic field last several such turnover times, after which the flows become statistically steady. In calculations with a magnetic field, the Joule dissipation is responsible for the larger part of the total dissipation rate [cf. Figs. 2(a), 2(c), 2(b), and 2(d)].

The DNS curves in Figs. 1 and 2 are obtained without prior filtering, i.e., they represent the full energy and dissi-

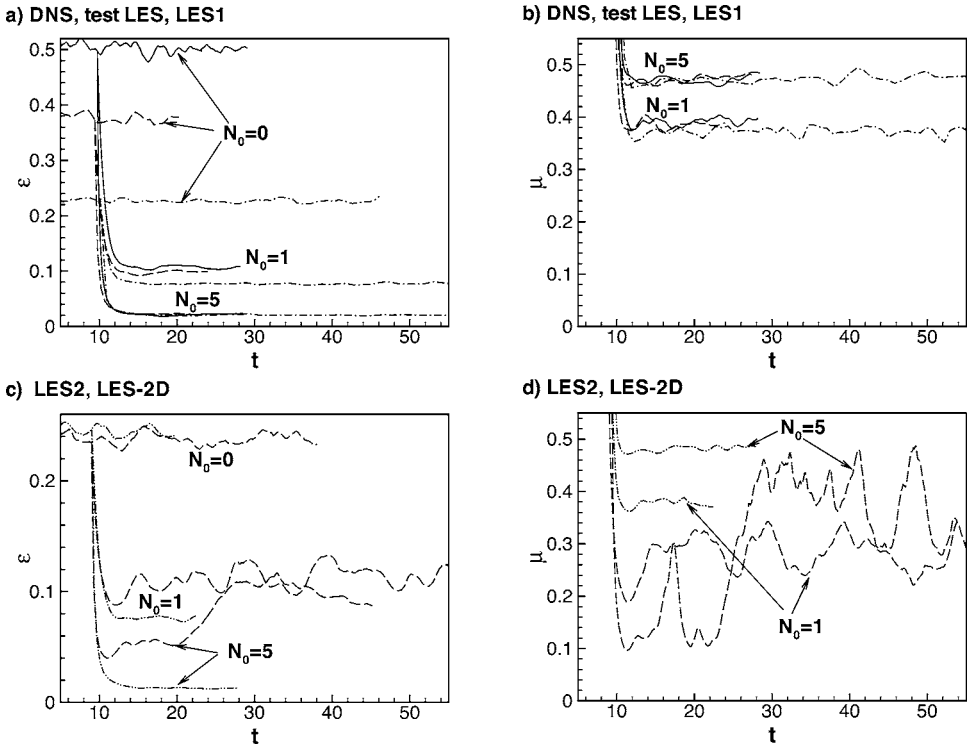

FIG. 2. Evolution of viscous [(a) and (c)] and magnetic [(b) and (d)] dissipation rates. DNS (—), test LES (-·-·-), and LES1 (– – –) are shown in (a) and (b). LES2 (-·-·-·-) and LES-2D (– – –) are shown in (c) and (d). For LES, only the resolved part of dissipation is plotted.

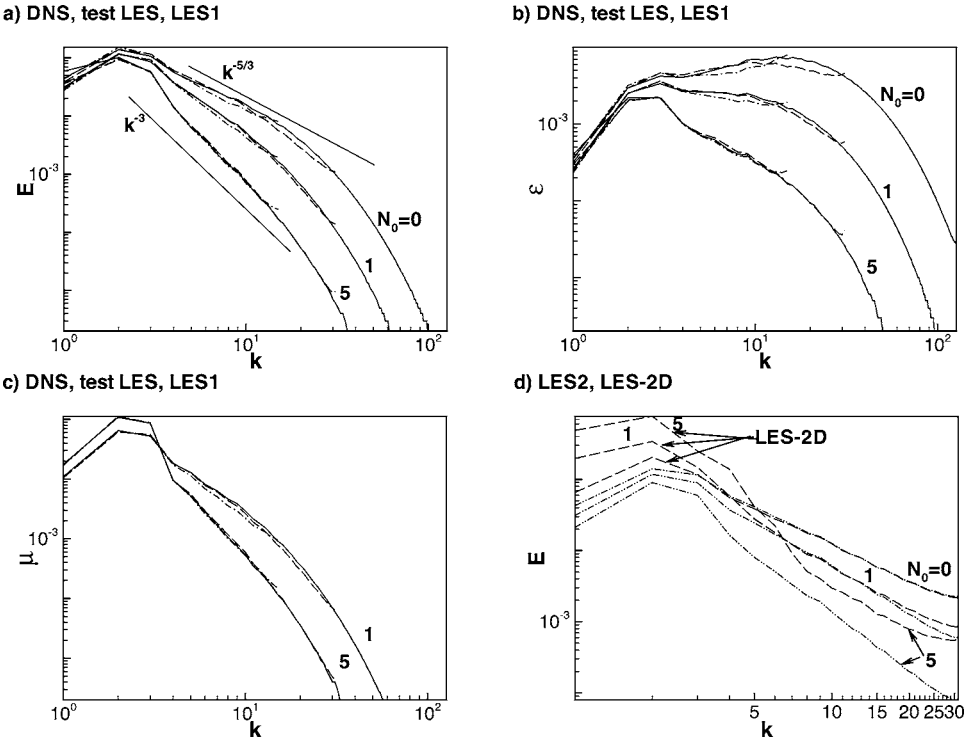

FIG. 3. (a)–(c) Comparison between DNS (—), test LES (-·-·-), and LES1 (– – –). Spectra of kinetic energy (a), viscous (b), and magnetic (c) dissipation are shown. (d) Spectra of kinetic energy for LES2 (-···-) and LES-2D (– – –).

pation rates of the flow. One can see in Fig. 1(a) that the total energy is quite close to that of the resolved scales in the test LES runs. This indicates that only a small fraction of the energy is contained in the subgrid scales, a fact that can also be seen in the energy and dissipation spectra shown in Fig. 3.

Increasing Re has virtually no effect on the flow energy [see Fig. 1(b)], which is not surprising. On the other hand, as illustrated in Fig. 1(c), applying the two-dimensional forcing results in completely different energy curves. As the flow becomes more anisotropic, its behavior becomes more dominated by a slow evolution of large-scale quasi-two-dimensional structures. This is particularly pronounced at $N_0=5$.

Another interesting observation can be made. At the same energy injection rate, the total energy decreases with N in the case of the three-dimensional forcing but increases if the forcing is two-dimensional [see Fig. 1(c)]. As can be seen in the power spectra in Fig. 3(d), these trends are due to the growth/decay of the energy of the large-scale modes. An explanation can be given as follows. In the case of the three-dimensional forcing, the Joule dissipation acts directly on all modes including the most energetic large-scale ones, into which energy is injected by forcing. A significant part of this energy is immediately dissipated into Joule heat. Larger N results in stronger dissipation and smaller energy.

The situation is quite different in the case of two-dimensional forcing, when the injection is limited to modes with $k_z=0$. As illustrated in Figs. 4(b) and 8(d), the large scales of the flow become strongly anisotropic at $N_0=1$ and almost two-dimensional at $N_0=5$. The Joule dissipation of energetic large-scale modes subsides. Furthermore, enhanced anisotropy hinders the energy transfer to smaller scales. As a result, the energy of the forced modes and of the entire flow grows with N.

This amplification of the large-scale quasi-two-dimensional structures at large N is reminiscent of the behavior of such flows as jets or strained vortices parallel to the imposed magnetic field. At weak or zero field, they become unstable, disintegrate, and lose their energy to increasing Joule dissipation. At a sufficiently large N, however, such flows are stabilized by the magnetic field and their energy remains large (see, e.g., Refs. 24 and 25 for a more detailed discussion of this phenomenon).

The viscous dissipation curves in Fig. 2(a) give us an opportunity to see how the role played by the SGS model changes in the presence of the magnetic field. As N increases, the difference between the DNS and test LES, which roughly corresponds to the SGS dissipation rate, becomes smaller. At the same energy injection rate and the same viscosity, the model is responsible for a smaller portion of the viscous dissipation and, thus, plays a smaller part in the flow evolution.

Our simulations show certain trends in the dependency of the asymptotic values of E, ϵ, and μ on the magnetic interaction parameter. They cannot, however, be used for developing or verifying universal scaling laws. First of all, as clearly shown by the comparison of LES2 and LES-2D solutions, such universal relations are impossible since the behavior of global characteristics is strongly influenced by the type of forcing. Here, the situation is different from that of the decaying turbulence, where the uncertainties associated with the forcing are avoided and the scaling laws can be developed.[5,7,10] Furthermore, our experiments taken in a small range of Re and at only three different values of N are insufficient to prove any scaling hypothesis.

Spectra of energy and viscous and magnetic dissipation rates were obtained at the equilibrium stages of each flow. Several velocity fields separated by, at least, one turnover

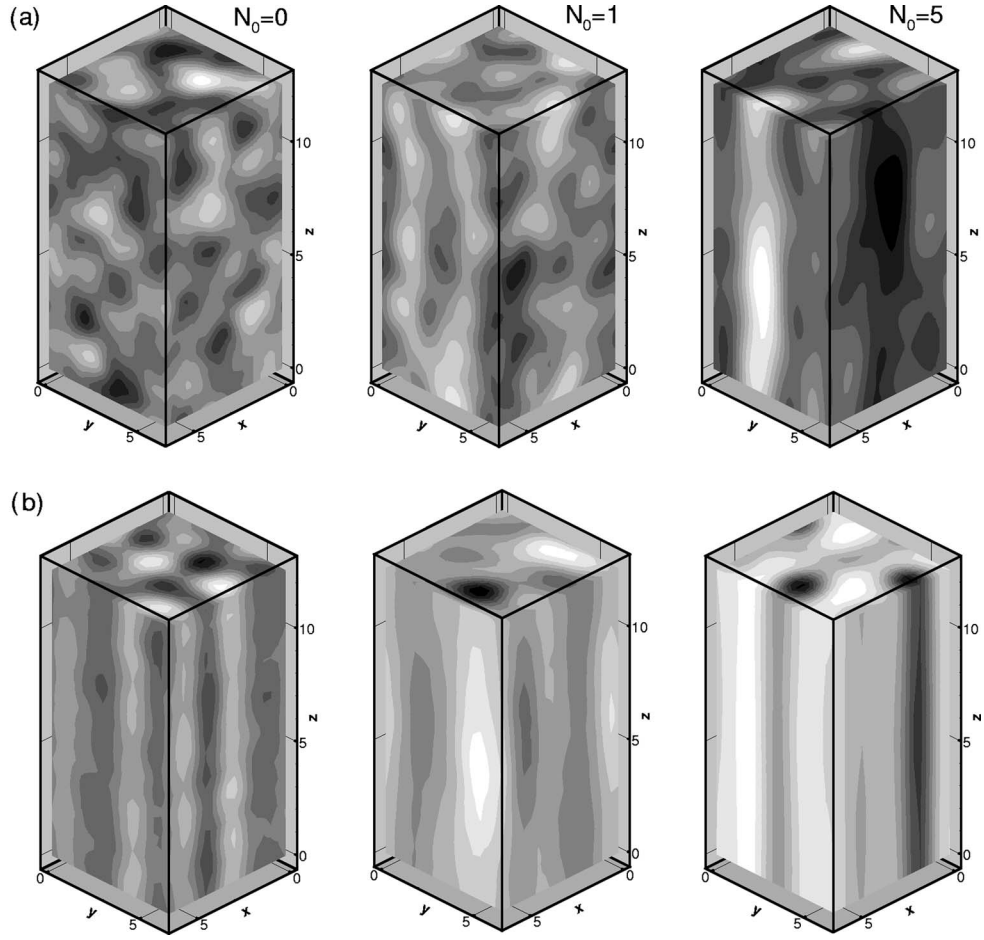

FIG. 4. Modified pressure fields in developed flows. (a) DNS, (b) LES-2D.

time from each other were used for averaging. One can see in Figs. 3(a)–3(c) that the spectra obtained in DNS, test LES, and LES1 are very close. This can be considered as an indication of the accuracy of the dynamic LES model. In the presence of the magnetic field, the energy spectra become steeper with a slope approaching k^{-3} at $N_0=5$. Comparison between the LES-2D and LES2 runs in Fig. 3(d) demonstrates strong differences at large scales but similar slopes at k sufficiently distant from the forced region.

The internal structure of the flow is illustrated in Fig. 4, where we plot snapshots of the modified pressure field Π_1 in developed flows. The pressure field is calculated using the Poisson equation,

$$\nabla^2\Pi_1 = \rho\,\nabla\cdot[\mathbf{v}\times\mathbf{w}], \tag{13}$$

and is defined as

$$\Pi_1 = p + \frac{1}{\mu}(\mathbf{B}\cdot\mathbf{b}) + \rho\frac{\mathbf{v}^2}{2}. \tag{14}$$

Here $\mathbf{w}=\nabla\times\mathbf{v}$ is vorticity, $\mathbf{B}=B_0\mathbf{e}_z$ is the imposed magnetic field, and $\mathbf{b}$ stands for the perturbation of the magnetic field induced by the fluid motion. We also assume that the density is $\rho=1$ in (13). Figures 4(a) and 4(b) demonstrate the difference between the structures of the large-scale eddies in the cases of three-dimensional and two-dimensional forcing. In the 3D case, the tendency to develop anisotropy in the presence of a magnetic field is clearly seen, although the flow is far from approaching a purely two-dimensional form even at $N_0=5$. On the contrary, the snapshots of the modified pressure in the flows with quasi-2D forcing in Fig. 4(b) show almost 2D structures for the run with strong magnetic field and strong anisotropy for the runs with $N=0$ and $N=1$.

III. ANISOTROPY

One has to distinguish between two types of anisotropy. One is the anisotropy of the Reynolds stress tensor or, in other words, the inequality between the components of the velocity field. In this paper, we refer to this as the velocity anisotropy. The other is the anisotropy of gradients, which characterizes the difference between the magnitudes of the derivatives of flow properties taken along and across the magnetic field direction. The Joule dissipation directly affects only the velocity gradients along the magnetic field lines, thus leading to the gradient anisotropy. The velocity anisotropy is a secondary effect, whose existence, strength, and relation to the intensity of the magnetic field are far from being obvious.

A. Integral characteristics

We start with the integral characteristics of the anisotropy of gradients[11,12]

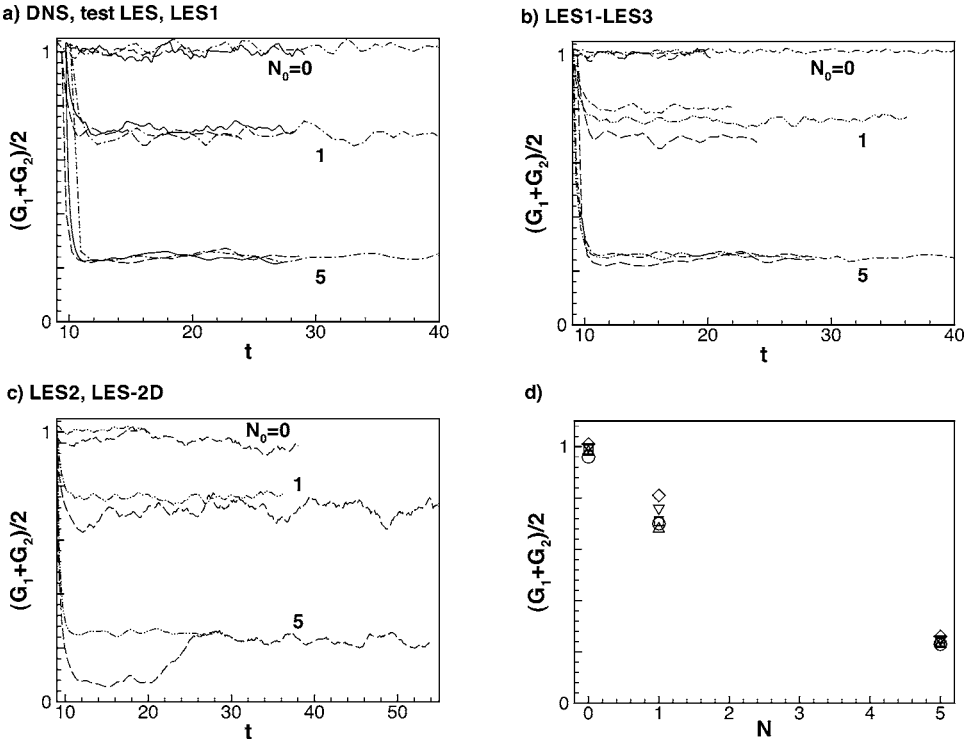

FIG. 5. Anisotropy coefficients $(G_1+G_2)/2$ given by (15). (a) DNS (—), test LES (-·-·-), and LES1 (– – –). (b) LES1 (– – –), LES2 (-···-), and LES3 (-·-·-). (c) LES2 (-···-) and LES-2D (– – –). (d) Time-averaged $(G_1+G_2)/2$ for DNS (□), LES1 (△), LES2 (▽), LES3 (◇), and LES-2D (○). Averaging is done for $30<t<50$ at $N=5$ in LES-2D.

$$G_1 = \frac{\langle(\partial v_2/\partial z)^2\rangle}{2\langle(\partial v_2/\partial y)^2\rangle} \quad \text{and} \quad G_2 = 2\frac{\langle(\partial v_3/\partial z)^2\rangle}{\langle(\partial v_3/\partial y)^2\rangle}. \tag{15}$$

The coefficients must be equal to 1 in a perfectly isotropic flow and 0 in a two-dimensional flow independent of the coordinate along the magnetic field lines. In a three-dimensional anisotropic flow, G_1 and G_2 are usually close to each other so the average $(G_1+G_2)/2$ is shown in Fig. 5.

After the introduction of the magnetic field, the anisotropy coefficients G_1 and G_2 quickly decrease and stabilize at statistically steady levels that correspond to a moderately anisotropic flow at $N_0=1$ and a strongly anisotropic but still three-dimensional flow at $N_0=5$. We do not observe an intermittent 2D laminar–3D turbulent behavior similar to that found in Ref. 12. The reason is the different forcing mechanism used in the present work. The energy input is equally divided between a large number of forced modes (212 in the case of the 3D forcing and 20 when the forcing is 2D). This prevents the development of a single dominating large-scale mode corresponding to a 2D laminar structure, which was an essential part of the intermittency observed in Ref. 12.

One can see in Fig. 5(a) that there is no noticeable difference between the coefficients (15) obtained in DNS and test LES. The dynamic model accurately reproduces the anisotropy of the resolved scales. Figure 5(b) illustrates the fact that, within the range of Re covered by LES1-LES3, the anisotropy of the gradients is virtually independent of the Reynolds number.

An interesting observation can be made in Fig. 5(c). The effect of the type of forcing is surprisingly weak. G_1 and G_2 calculated in LES-2D eventually stabilize at the levels close to those obtained in the 3D forcing counterpart LES2. This appears counterintuitive since it is clear that additional anisotropy is introduced by the two-dimensional forcing in comparison with the three-dimensional case. Furthermore, the result is in seeming contradiction with Fig. 4, where the LES-2D flows look much more anisotropic than the flows obtained with the three-dimensional forcing. An explanation is based on the fact that the values of G_1 and G_2 are calculated with squares of velocity gradients and, thus, are dominated by the intermediate and small scales, while the pressure fields in Fig. 4 primarily reflect the shape of the large-scale modes of the flow. We will show below that the anisotropy of intermediate and small length scales is only weakly influenced by the type of the forcing and the Reynolds number.

The results are summarized in Fig. 5(d), where we show the time-averaged values of $(G_1+G_2)/2$ obtained by averaging over the periods of statistically steady evolution of fully developed flows. It is clearly seen that the integral anisotropy characteristics G_1 and G_2 are predominantly functions of the magnetic interaction parameter N only slightly affected by Re and large-scale dynamics.

One aspect of the velocity anisotropy has to be mentioned before we proceed with the discussion of our results. In the axisymmetric case such as ours, the anisotropy can appear in two different forms. The velocity component in the preferred direction can be either stronger or weaker than the two perpendicular components (so-called prolate axisymmetric or oblate axisymmetric states). Which form actually occurs depends on specific organization of the flow, boundary conditions, etc. For the decaying homogeneous MHD turbulence, the linearized model[5] valid for $N \gg 1$ predicts that the flow is "channeled in the **B** direction" so that the kinetic energy E_3 of the parallel velocity component is equal to the sum of the energies E_1 and E_2 of the two perpendicular components. Completely different evolution was observed in the

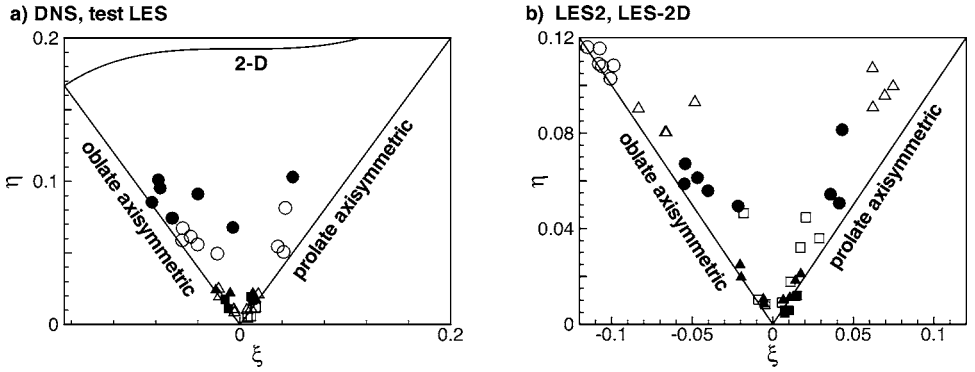

FIG. 6. Invariant maps of velocity anisotropy tensor (16) in fully developed flows. Squares, triangles, and circles are for $N_0=0$, 1, and 5, correspondingly. (a) DNS (filled symbols) and test LES (unfilled symbols). (b) LES2 (filled symbols) and LES-2D (unfilled symbols).

forced homogeneous turbulence. Strongly anisotropic flow that developed in the presence of an artificial large-scale forcing had the form of columnar vortices with axes parallel to the magnetic field and motion primarily in the perpendicular plane, i.e., with $E_3 \ll E_1, E_2$.[12] On the contrary, in turbulent convection driven by a constant temperature gradient, E_3 grew and became dominant when a strong parallel magnetic field was applied.[24]

The velocity anisotropy can be evaluated with the help of the traceless tensor

$$b_{ij} = \frac{\langle v_i v_j \rangle}{\langle v_k v_k \rangle} - \frac{1}{3}\delta_{ij}, \tag{16}$$

which has two nontrivial invariants $6\eta^2 = b_{ij}b_{ji}$ and $6\xi^3 = b_{ij}b_{jk}b_{ki}$.[26] The magnitude of η represents the degree of anisotropy, while the sign of ξ shows its type ("pencil-like" flows dominated by the parallel component or "pancake-like" dominated by the two perpendicular components at positive and negative ξ, respectively).

The invariants η and ξ calculated for developed flows at several moments separated from each other by a few eddy turnover times are shown in Fig. 6. If proper ensemble averaging were applied, the matrix b_{ij} would accept one of the two forms characteristic for axisymmetric turbulence, i.e., would be purely diagonal with a single positive or negative anisotropy constant α such that $b_{11}=b_{22}=\alpha$, $b_{33}=-2\alpha$, $\eta = |\alpha|$, and $\xi=-\alpha$ (lines corresponding to prolate and oblate axisymmetric states in Fig. 6). In our simulations, η and ξ obtained by volume averaging fluctuate strongly, demonstrating strong deviations of the flow from the purely axisymmetric states. An explanation can be given based on the fact that, unlike the case of G_1 and G_2, the main contribution to the components of tensor b_{ij} comes from the large-scale modes. These modes experience slow (at the time scale $T \sim 1$) chaotic evolution governed by the interaction between the modes and by forcing. At any particular moment, there can be significant disparity between the energies of the two perpendicular velocity components of these dominating modes and, thus, of the entire flow, as reflected by Fig. 6.

In the case of the three-dimensional forcing, the velocity field is fairly isotropic at $N_0=0$ and $N_0=1$. The flow with strong magnetic field ($N_0=5$) demonstrates a degree of anisotropy, with the velocity field being more often dominated by the perpendicular velocity components than by the parallel component. Figure 6(a) also shows a qualitative agreement between the anisotropy in DNS and test LES simulations. Figure 6(b) demonstrates that, when the forcing is limited to the modes with $\mathbf{k} \perp \mathbf{B}$, a substantial anisotropy develops even at $N_0=0$. At $N_0=5$, the LES-2D velocity field is clearly dominated by the two perpendicular velocity components. Combining this with the observation of the columnar structures seen in Fig. 4, we may conclude that the flow tends to organize itself into a pattern of vortices with axes parallel to the magnetic field and streamlines in perpendicular planes, which is reminiscent of the pattern found at large N in Ref. 12.

B. Anisotropy at different length scales

We now approach the question of the length-scale dependence of the anisotropy formulated in the beginning of this paper. The following discussion is based on the DNS and LES performed at moderate Reynolds numbers and with moderate numerical resolution. Since the range of the active length scales available to us is not very large ($1<k<128$ in the DNS and $1<k<64$ in the highest resolution LES), the results should not be considered as proof of a certain scale behavior in a high-Re turbulence but rather as an indication of a trend that can be carefully extrapolated into a more general conclusion.

We used the computed energy spectra to evaluate the magnetic interaction parameters corresponding to different

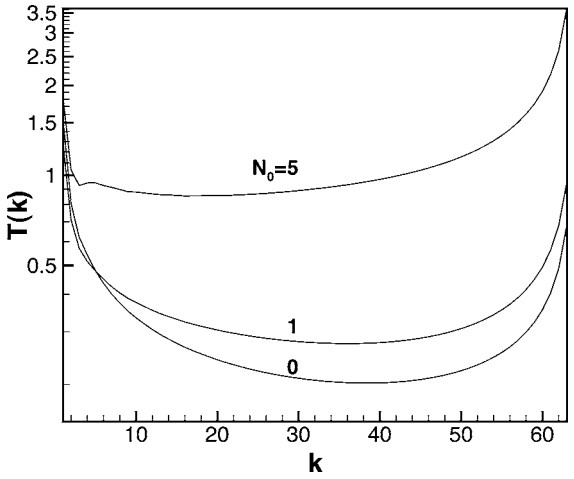

FIG. 7. Scale-dependent eddy turnover time $T(k)$ as a function of the wave number. Curves corresponding to $N_0=0$, 1, and 5 are shown for LES4.

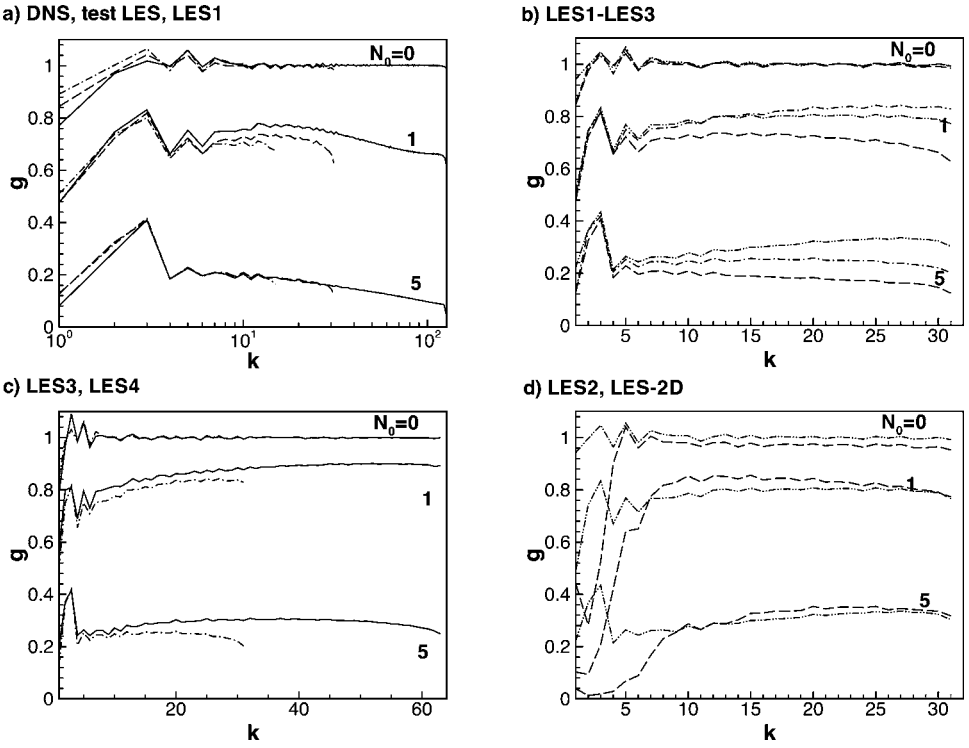

FIG. 8. Anisotropy of the gradient anisotropy coefficient (17) as a function of k. (a) DNS (—), test LES (-·-·-), and LES1 (– – –). (b) LES1 (– – –), LES2 (-··-··-), and LES3 (-·-·-). (c) LES3 (-·-·-) and LES4 (—). (d) LES2 (-··-··-) and LES-2D (– – –).

length scales. For each simulation, the scale-dependent eddy turnover time $T(k)=1/kv(k)=N(k)\rho/\sigma B^2$ was calculated, where $v(k)\approx[(2/3)\int_k^{k_{\max}}E(k)dk]^{1/2}$ is the typical velocity of a turbulent eddy of the size $\ell=1/k$. In the inertial range at high Re, $T(k)\sim k^{-2/3}$. At the modest Re of our simulations, we found that the typical ratio between the maximum and minimum values of $N(k)$ was about 3 or 4. For example, in the case of LES4 illustrated in Fig. 7, this ratio is approximately 3.4 for $N_0=0$ and $N_0=1$ and 4.2 for $N_0=5$. In the previous section, we saw that a comparable variation of the integral interaction parameter between the runs resulted in a significant difference in the degree of the flow anisotropy. What remains to be seen is whether such a difference can be found in a single run at different length scales.

We start with the anisotropy of gradients. It was found in earlier DNS[12] that the steepening of the energy spectrum with growing N was closely followed by the steepening of the Joule dissipation spectrum. This behavior is confirmed by our simulations for larger Reynolds numbers and a different forcing (see Fig. 3 for an illustration). The ratio

$$g(k)\equiv\frac{3\tau}{2}\frac{\mu(k)}{E(k)}=\frac{3\sum\frac{k_z^2}{k^2}\hat{\mathbf{u}}\cdot\hat{\mathbf{u}}^*}{\sum\hat{\mathbf{u}}\cdot\hat{\mathbf{u}}^*}=\frac{3D_{33}(k)}{2E(k)} \tag{17}$$

can be considered as a measure of the gradient anisotropy at the wavelength $1/k$. In (17), the sums are over all wavenumber vectors in the shell $k-1/2<|\mathbf{k}|\leqslant k+1/2$ and D_{33} is a component of the dimensionality tensor.[27] The scaling factor is chosen so that $g(k)=1$ in isotropic flows. In purely two-dimensional flows with zero magnetic dissipation, $g(k)=0$.

Several important observations can be made on the basis of the simulation results presented in Fig. 8. First of all, in all experiments, there are significant ranges of length scales in which $g(k)$ varies only slightly with k. Each such range begins almost immediately outside the forced region and extends to the smallest resolved length scales. The values of $g(k)$ are close to the values of the integral coefficients G_1 and G_2 (cf. Fig. 5). This was observed in all our simulations including those with the two-dimensional forcing. In some LES runs, $g(k)$ seems to vary faster when k approaches the cutoff $k_{\max}$. This is, probably, an artefact due to the SGS closure and de-aliasing procedure. A confirmation is in Fig. 8(c), where we compare the results of LES3 with the results of LES4 performed at the same Re and N_0 but with double $k_{\max}$. Shifting the LES filter to smaller scales results in a corresponding extension of the range where $g(k)$ is scale independent. It is important to note that this range covers the scales corresponding, according to Fig. 7, to the values of the scale-related magnetic interaction parameter varying by a factor of 3, at least. The values of $g(k)$ in the scale-independent region are close to the values of G_1 and G_2 shown in Fig. 5. We can conclude that the integral anisotropy coefficients are good indicators of the anisotropy of turbulent fluctuations in a wide range of small and moderate scales.

It can also be seen that the anisotropy in this range is primarily determined by the value of the magnetic interaction parameter. $g(k)$ does show the tendency to increase slightly with Re but this effect is much weaker than the effect of N. Curiously, there is little sensitivity to the type of forcing, as seen in Fig. 8(d). Within the forced region, where the gradient anisotropy is directly introduced by the two-dimensional forcing, $g(k)$ in LES-2D is about two times smaller than in LES2. Outside of this region, however, the two curves converge quickly and become close to each other for all three values of N_0. The visually different flows ob-

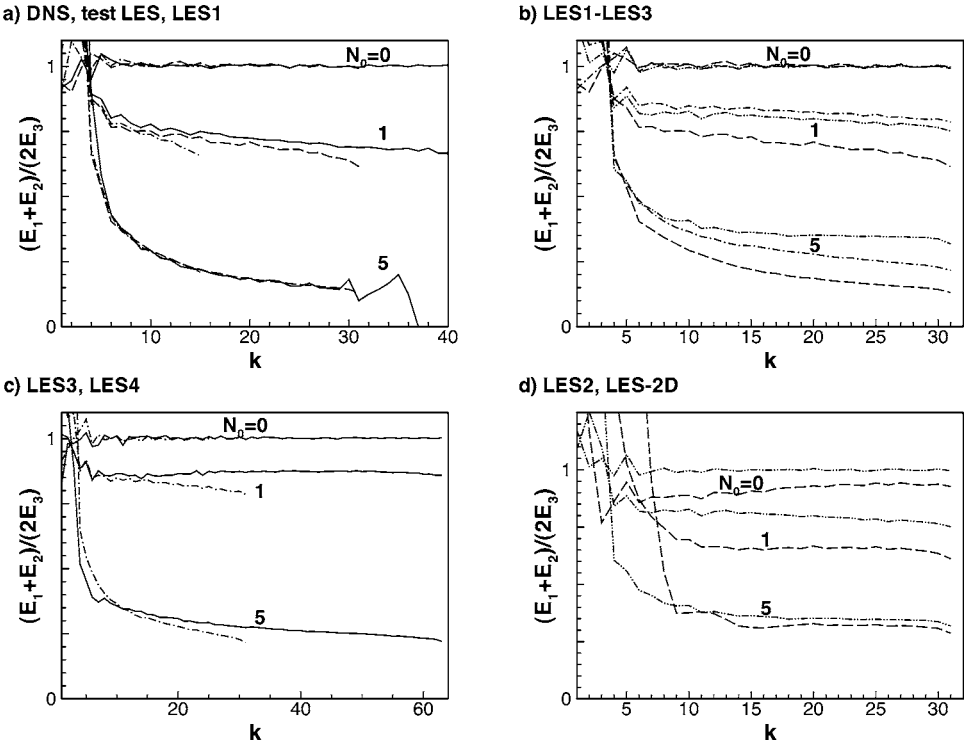

FIG. 9. Velocity anisotropy coefficient $c(k)$ given by (18). Notation is as in Fig. 8.

tained with isotropic and two-dimensional forcing mechanisms [cf. Figs. 4(a) and 4(b)] possess, for the same strength of the magnetic field, similar degrees of anisotropy of small-scale turbulent fluctuations.

Finally, one can see in Fig. 8(a) that there is a good agreement between the DNS and test LES results.

To analyze the velocity anisotropy, we calculate the ratio of the typical energies of the parallel and perpendicular velocity components at different length scales. Figure 9 shows

$$c(k) = \frac{E_1(k) + E_2(k)}{2E_3(k)}, \tag{18}$$

where

$$E_i(k) = \frac{1}{2} \sum_{k-1/2<|\mathbf{k}|<k+1/2} [v_i(\mathbf{k}) \cdot v_i^*(\mathbf{k})], \quad i = 1,2,3. \tag{19}$$

The scale dependence of the velocity anisotropy can be described in terms similar to those used for the gradient anisotropy. We see in Fig. 9 that, outside of the forced region, the coefficient $c(k)$ varies only slightly with k for all values of N. Comparison between the curves for LES3 and LES4 in Fig. 9(c) shows that the extension of the resolved scale range leads to an extension of the subrange, where the anisotropy is approximately constant.

As shown in Fig. 9(b), the Reynolds number does not seriously affect the velocity anisotropy. We also see that the conclusion that could be made from Fig. 6(a), about the predominance of structures with $E_1, E_2 > E_3$, is correct only in regard to the large energy containing scales. For smaller scales, the tendency is reversed. The velocity component along the magnetic field lines becomes stronger than the perpendicular components. The observation that the large-scale velocity anisotropy is not necessarily followed by a similar anisotropy at small scales is supported by the comparison between the LES2 and LES-2D curves in Fig. 9(d). Even though there is a difference between the curves for $N_0=0$ and $N_0=1$, the strength of the magnetic field is the dominant factor determining the value of $c(k)$ at nonforced scales. This conclusion can be viewed as suggesting that in different turbulent flows such as, for example, a channel flow in a perpendicular magnetic field,[6] where $v_z < v_x, v_y$, or a jet stabilized by a longitudinal magnetic field,[13,24] where $v_z > v_x, v_y$, the velocity anisotropy of small-scale fluctuations is of a prolate axisymmetric kind and determined predominantly by the magnetic interaction parameter rather than by the particular flow conditions.

IV. CONCLUSIONS

Direct numerical and large-eddy simulations of forced homogeneous turbulence in a low-Re_m MHD flow have been performed. Three different values of the magnetic interaction parameter corresponding to zero, moderate, and strong applied magnetic fields are investigated. The anisotropy of flow gradients and velocity components is analyzed using integral and scale-dependent characteristics.

Both types of anisotropy are found to vary only slightly with the length scale outside the range of the large-scale energy-containing modes. This is an important new result that could not be derived from existing theoretical models, experimental data, or general physical considerations. A word of caution must be given that our observation is based on moderate-Re simulations and does not contradict Kolmogorov's hypothesis that the small scales become isotropic at sufficiently large Re. Rather, our conclusion is that even when the magnetic interaction parameter varies substantially

with the length scale, the change in the degree of anisotropy remains small, much smaller than the change associated with a similar variation of N at the global level.

LES performed at different Reynolds numbers in the range $300 \leqslant \mathrm{Re} \leqslant 2600$ show that the effect of Re on the anisotropy is weak.

The gradient and velocity anisotropies caused by the large-scale forcing are observed only at the scales close to the forced region. At smaller scales, the effect of the large-scale dynamics on turbulent fluctuations quickly subsides.

To summarize, our simulations indicate that the anisotropy of low-Re_m MHD turbulence at the scales outside the energy-containing range is predominantly a function of the magnetic interaction parameter. The effects of scale, hydrodynamic Reynolds number, and the details of the large-scale dynamics are much weaker.

The work also confirms the earlier conclusion[19] that the dynamic Smagorinsky model provides an effective approach to the simulation of anisotropic MHD turbulence. Indeed, *a posteriori* testing of the model based on the comparison between DNS and LES has consistently shown a good agreement for the flow characteristics such as energy spectra, viscous and magnetic dissipation rates, and the anisotropy of the resolved scales.

Although not directly related to any of the technological processes mentioned in the Introduction, our results provide a better understanding of the properties of anisotropic MHD turbulence at low Re_m and move us closer to developing accurate and physically sound numerical models of liquid metal flows. Moreover, our validation of the dynamic Smagorinsky model at moderate Re is of direct importance for future simulations of at least one process, growth of large silicon crystals by the Czochralski method, which is characterized by moderate values of Re and N.

ACKNOWLEDGMENTS

Part of this work was performed during the 2004 Summer Program organized by the Center for Turbulence Research at Stanford University and NASA Ames Research Center. The authors would like to thank P. Moin and N. Mansour for their hospitality during the stay. The authors have benefited from numerous fruitful discussions with A. Thess, R. Moreau, S. Kassinos, and D. Carati. The work of A.V. and O.Z. was supported by Grant No. DE FG02 03 ER46062 from the U.S. Department of Energy and by Grant No. INT 0338713 from the U.S. National Science Foundation. The computations were performed on the parallel computer cluster at the University of Michigan–Dearborn, acquired with the support of Grant No. CTS 0320621 from the MRI program of the National Science Foundation.

[1] R. Moreau, *Magnetohydrodynamics* (Kluwer Academic, Dordrecht, 1990).
[2] P. A. Davidson, *An Introduction to Magnetohydrodynamics* (Cambridge University Press, Cambridge, 2001).
[3] J. Cho, A. Lazarian, and E. T. Vishniac, "MHD turbulence: Scaling laws and astrophysical applications," in *Turbulence and Magnetic Fields in Astrophysics*, Vol. 614 of Lecture Notes in Physics, edited by T. Passot and E. Falgarone (Springer, New York, 2003), p. 56.
[4] B. Knaepen, S. Kassinos, and D. Carati, "Magnetohydrodynamic turbulence at moderate magnetic Reynolds number," J. Fluid Mech. **513**, 199 (2004).
[5] H. K. Moffatt, "On the suppression of turbulence by a uniform magnetic field," J. Fluid Mech. **28**, 571 (1967).
[6] J. Sommeria and R. Moreau, "Why, how, and when, MHD turbulence becomes two-dimensional," J. Fluid Mech. **118**, 507 (1982).
[7] P. A. Davidson, "The role of angular momentum in the magnetic damping of turbulence," J. Fluid Mech. **336**, 123 (1997).
[8] P. A. Davidson, "Magnetohydrodynamics in materials processing," Annu. Rev. Fluid Mech. **31**, 273 (1999).
[9] A. D. Votsish and Yu. B. Kolesnikov, "Investigation of transition from three-dimensional turbulence to two-dimensional under a magnetic field," Magnetohydrodynamics (N.Y.) **3**, 141 (1976).
[10] A. Alemany, R. Moreau, P. L. Sulem, and U. Frisch, "Influence of external magnetic field on homogeneous MHD turbulence," J. Mec. **18**, 280 (1979).
[11] U. Schumann, "Numerical simulation of the transition from three- to two-dimensional turbulence under a uniform magnetic field," J. Fluid Mech. **74**, 31 (1976).
[12] O. Zikanov and A. Thess, "Direct numerical simulation of forced MHD turbulence at low magnetic Reynolds number," J. Fluid Mech. **358**, 299 (1998).
[13] O. Zikanov and A. Thess, "Direct numerical simulation as a tool for understanding MHD liquid metal turbulence," Appl. Math. Model. **28**, 1 (2004).
[14] The process of the development of anisotropy can be viewed from a different angle. In particular, a description based on the fact that the Lorentz force conserves the component of angular momentum parallel to the magnetic field was proposed (Ref. 7).
[15] F. S. Godeferd, L. Liechtenstein, and C. Cambon, "Parametric analysis of anisotropy in stably stratified rotating homogeneous turbulence," in *Turbulence and Shear Flow Phenomena*, Proceedings of the 4th International Symposium, edited by J. A. C. Humphrey *et al.* (2005), Vol. 1, p. 343.
[16] S. G. Saddoughi and S. V. Veeravalli, "Local isotropy in turbulent boundary layers at high Reynolds number," J. Fluid Mech. **268**, 333 (1994).
[17] A. Pumir and B. I. Shraiman, "Persistent small scale anisotropy in homogeneous shear flows," Phys. Rev. Lett. **75**, 3114 (1995).
[18] L. Biferale, I. Daumont, A. Lanotte, and F. Toschi, "Theoretical and numerical study of highly anisotropic turbulent flows," Eur. J. Mech. B/Fluids **23**, 401 (2004).
[19] B. Knaepen and P. Moin, "Large-eddy simulation of conductive flows at low magnetic Reynolds number," Phys. Fluids **16**, 1255 (2004).
[20] M. Germano, U. Piomelli, P. Moin, and W. H. Cabot, "A dynamic subgrid-scale eddy viscosity model," Phys. Fluids A **3**, 1760 (1991).
[21] D. K. Lilly, "A proposed modification to the Germano subgrid-scale closure model," Phys. Fluids A **4**, 633 (1992).
[22] J. H. Williamson, "Low-storage Runge-Kutta schemes," J. Comput. Phys. **35**, 48 (1980).
[23] R. Rogallo, "Numerical experiments in homogeneous turbulence," NASA Technical Memorandum 81315, NASA, Ames Research Center (1981).
[24] O. Zikanov, A. Thess, and J. Sommeria, "Turbulent convection driven by an imposed temperature gradient in the presence of a constant magnetic field," in *Notes on Numerical Fluid Mechanics*, edited by E. H. Hirschel (Vieweg, Wiesbaden, 1998), Vol. 66, 187.
[25] A. Thess and O. Zikanov, "On the transition from two-dimensional to three-dimensional MHD turbulence," in *Studying Turbulence Using Numerical Databases—X*, Proceedings of the 2004 CTR Summer Program (Center for Turbulence Research, Stanford, CA, 2004), p. 63.
[26] J. L. Lumley and G. R. Newman, "The return to anisotropy of homogeneous turbulence," J. Fluid Mech. **82**, 161 (1977).
[27] S. C. Kassinos, W. C. Reynolds, and M. M. Rogers, "One-point turbulence structure tensors," J. Fluid Mech. **428**, 213 (2001).